April 2013

Bardet-Biedl Syndrome 2 (BBS2) Depletion Affects Primary Cilia in Pancreatic Islets and Glucose Homeostasis

Lauren Elisabeth Harris
Worcester Polytechnic Institute

MQP-BIO-DSA-2312

BARDET-BIEDL SYNDROME 2 (BBS2) DEPLETION AFFECTS PRIMARY CILIA IN PANCREATIC ISLETS AND GLUCOSE HOMEOSTASIS

A Major Qualifying Project Report

Submitted to the Faculty of the

WORCESTER POLYTECHNIC INSTITUTE

in partial fulfillment of the requirements for the

Degree of Bachelor of Science

in

Biology and Biotechnology

by

Lauren Harris

April 25, 2013

APPROVED:

Agata Jurczyk, PhD
Molecular Medicine
UMass Medical School
MAJOR ADVISOR

David Adams, PhD
Biology and Biotechnology
WPI Project Advisor

ABSTRACT

Bardet-Biedl Syndrome (BBS) is a pleiotropic ciliopathy characterized by a unique phenotype including obesity, type II diabetes, polydactyly, cognitive deficiency, and blindness. The high prevalence of obesity (70-90%) and diabetes (up to 48%) among BBS patients has drawn attention to the disease as a way to discover previously unknown biochemical and developmental pathways connected to the disease's phenotypic manifestations. Immunofluorescence staining and perifusion showed low levels of insulin in pancreatic islets of BBS2 knockout mice. Glucose tolerance testing showed glucose intolerance, and insulin tolerance testing showed insulin resistance among BBS2 knockout mice, indicating the potential for disregulation of glucose homeostasis as a result of BBS2 depletion. Primary cilia in pancreatic islets were examined because BBS is a ciliopathy, and a unique phenotype of atypically short cilia was observed in BBS2 knockouts. BBS2 knockdown was accomplished *in vitro* and showed lower insulin levels, supporting the previous findings that loss of BBS2 leads to low insulin levels. The link between BBS and obesity led to examining the canonical *wnt* signaling pathway, a known adipogenesis repression pathway. Several canonical *wnt* genes were seen to be downregulated as a result of BBS2 knockdown. The *wnt* target gene Cyclin D1 is a cell cycle progression marker and it was also downregulated. Cell cycle analysis showed s-phase arrest during BBS2 knockdown. Both the *in vivo* and *in vitro* experiments pointed to the importance of BBS2 for normal glucose homeostasis, and provided a new model for diabetes research.

TABLE OF CONTENTS

ACKNOWLEDGEMENTS

I would like to thank Agata Jurczyk, PhD for guiding me and teaching me throughout the course of this project. She was incredibly helpful throughout this entire process, from teaching me how to perform all of the techniques used to helping me interpret the results of various tests editing the final paper. Thanks to Dale Greiner, PhD for allowing me to work in his lab and setting up my project with Agata. I would not have succeeded without the help of Linda Leehy and Linda Paquin who performed all of the mouse work involved in this project. Additional thanks to Anetta for genotyping the mice. In addition I would like to thank Dr. Val Sheffield for generously providing the BBS2 knockout mice used. Last but not least, I would like to thank Professor David Adams for helping to set up this project, advise me along the way, and edit the final report.

BACKGROUND

Primary Cilia

Most cells in the human body contain a solitary cilium extending from the cell membrane into the extracellular environment. These cilia have come to be known as primary cilia, and they are typically immotile organelles found in almost every type of cell in the human body (Pedersen, et al., 2008; Wheatley, et al., 1996; Yokoyama, 2004). Cells grow primary cilia when they enter the G_0 phase of the growth cycle, and there are three stages of cilia formation, as shown in **Figure 1** (Pedersen, et al., 2008). The first stage occurs when a centriolar vesicle derived from the cell's Golgi apparatus attaches to a mother centriole. The centriolar vesicle invaginates, creating a pocket for the axoneme, which emerges from the centriole. In the second stage, secondary centriolar vesicles join with the original centriolar vesicle to accommodate the growing axoneme; during this stage, microtubule pairs form along the axoneme. The third stage of primary cilia formation occurs when the centriolar vesicle fuses with the cell membrane and the primary cilia is able to extend out into the extracellular environment (Pedersen, et al., 2008).

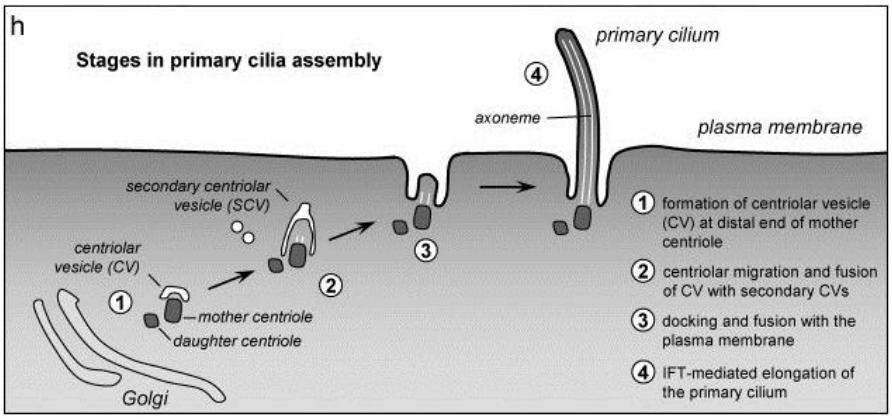

Figure 1: The stages of primary cilia assembly (Pedersen, et al., 2008).

Primary cilia are defined by their unique 9 + 0 structure in which there are nine microtubule triplets arranged in a circle in the cilium. Unlike motile cilia, primary cilia lack the central microtubule pair necessary for cilia mobility (Wheatley, et al., 1996; Yokoyama, 2004). Primary cilia can vary greatly in length, but a study by Wheatley and Bowser on kidney epithelial cells shows that cell populations typically have cilia length frequency distributions reminiscent of a bell curve. Their study showed primary cilia tended to be around 10.5 microns in length, and their histogram has been included as **Figure 2** (Wheatley, et al., 2000).

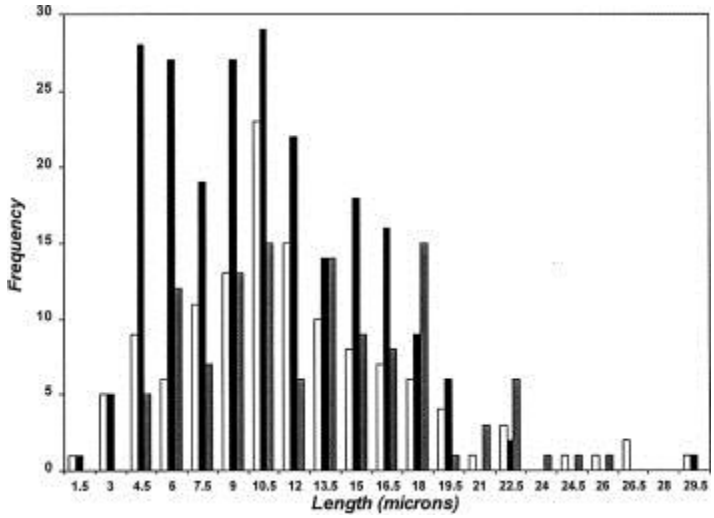

Figure 2: Histogram of primary cilia lengths in a kidney cell line showing the approximate length distribution of wild type primary cilia (Wheatley, et al., 2000).

Due to their prevalence and based on the disorders in which they are disrupted, primary cilia are widely believed to be involved in cell signaling, left-right asymmetry and development, and tissue formation and homeostasis (Pedersen, et al., 2008; Yokoyama, 2004; Christensen, et al., 2007). The role of primary cilia as sensory organelles makes them important in cell signaling. In the kidneys primary cilia have been shown to function as mechanosensors involved in monitoring urine composition and flow

rate (Christensen, et al., 2007). They have also been shown to coordinate platelet-derived growth factor receptor-alpha (PDGFRα) mediated signaling, which is involved in cell survival regulation, apoptosis, proliferation, migration, and angiogenesis (Christensen, et al., 2007).

A special kind of motile primary cilia has also been linked to left-right asymmetry during development. During development, primary cilia on node cells move to create nodal flow, which moves extracellular fluid from the right to the left. When nodal cilia were mutated so that they were either missing or immotile, left-right asymmetry didn't occur and situs inversus, physiological symmetry along the midline, was observed (Yokoyama, 2004). Additionally, studies where primary cilia were mutated showed disrupted Hedgehog and Gli protein regulation, both of which are essential for left-right asymmetry (Christensen, et al., 2007).

In addition to their role in development, primary cilia are also crucial for tissue formation and homeostasis. Primary cilia were shown to be necessary for proper forebrain development due to their role in proteolytic processing of the Gli3 transcription factor (Willaredt, et al., 2008). Then, in another study, mice with disrupted primary cilia showed pancreatic defects such as pancreatic duct expansion, cyst formation, and acinar cell apoptosis as well as renal cysts (Cano, et al., 2004). Primary cilia also play a role in photoreception and olfaction. For olfaction to occur, odorants must react with G Protein Coupled Receptors found on cilia membranes, and the presence of various olfactory signaling receptors in cilia indicates that cilia are crucial for odorant reception and signaling. Similarly, photoreception is also dependent on cilia signaling pathways. Both

rods and cones have primary cilia which are necessary for light reception and transduction (Singla, et al., 2006).

Ciliopathies

The wide variety of primary cilia functions and the importance of these functions show just how essential this organelle is. Any disruptions in primary cilia formation greatly affect their ability to function, as can be seen in ciliopathies. Ciliopathies are a group of human disorders associated with defects in cilia structure and function and which share several clinical phenotypes (Badano, et al., 2006). The nine phenotypes used to identify ciliopathies include retinitis pigmentosa, renal cystic disease, polydactyly, situs inversus, mental retardation and developmental delay, agenesis of the corpus callosum, Dandy-Walker malformation, posterior encephalocele, and hepatic disease. Retinitis pigmentosa occurs with the degeneration of photoreceptor cells, especially rods, which over time lose their ability to function (Saade, et al., 2013). Renal cystic disease occurs when cysts form in the kidneys (Badano, et al., 2006), and polydactyly is the presence of extra digits, which typically presents as extra fingers. As mentioned above, situs inversus occurs when left-right asymmetry is disrupted and the body is anatomically symmetric across the midline. Agenesis (hypoplasia) of the corpus callosum is underdevelopment of the band of nerve fibers that connect the left and right hemispheres of the brain. Dandy-Walker malformation is a syndrome in which the cerebellar vermis is underdeveloped, the fourth ventricle displays cystic dilation, and the posterior fossa is enlarged (Hamid, 2007). Posterior encephalocele occurs when the posterior lobe of the brain protrudes through a fissure in the skull.

From the above list of clinical features, eleven disorders have been identified as being due to cilia dysfunction. These diseases are the ciliopathies, and they include

Bardet-Biedl Syndrome (BBS), nephronophthisis (NPHP), Senior-Løken Syndrome (SNLS), Alström Syndrome (ALMS), Meckel-Gruber Syndrome (MKS), Joubert syndrome (JBTS), oral-facial-digital Syndrome (OFD 1), Jeune asphyxiating thoracic dystrophy (JATD), Ellis-van Creveld Syndrome (EVC), Leber congenital amaurosis (LCA), and Polycystic Kidney Disease (PKD) (Baker, et al., 2009).

Bardet-Biedl Syndrome (BBS)

Bardet-Biedl Syndrome (BBS) is a pleiotropic, autosomal recessive ciliopathy (Forsythe, et al., 2013). The major and minor phenotypic characteristics used to diagnose BBS are listed in **Table 1**, and a positive BBS diagnosis is based on the presence of either four major characteristics or three major characteristics and two minor characteristics. It is also recommended that a positive BBS diagnosis or a suspected case of BBS be confirmed by molecular genetic testing (Forsythe, et al., 2013; Baker, et al., 2009).

Table 1: The major and minor characteristics used to diagnose BBS (Forsythe, et al., 2013; Baker, et al., 2009).

Major Characteristics	Frequency
Rod-Cone Dystrophy	93%
Post-Axial Polydactyly	63-81%
Obesity	72-92%
Genital Anomalies	59-98%
Renal Anomalies	53%
Learning Difficulties	61%

Minor Characteristics	Frequency
Speech Delays	54-81%
Developmental Delays	50-91%
Diabetes Mellitus	6-48%
Dental Anomalies	51%
Congenital Heart Disease	7%
Brachydactyly/Syndactyly	46-100%/8-95%
Ataxial/Poor Coordination	40-86%
Anosmia/Hyposmia	60%
Loss of Nociception/ Thermosensation	–

The BBS phenotype appears over the first decade of life, but there is considerable phenotypic variance among BBS patients (Forsythe, et al., 2013). Rod-cone dystrophy is highly prevalent in BBS, and most BBS patients are legally blind by the age of 20-30

years old. First the rods degenerate, leading to night blindness and the development of photophobia; after this the cones are typically affected, and both color and central vision are lost. Post-axial polydactyly is also highly prevalent among BBS patients, and the *in utero* presence of extra fingers and toes is one of the earliest detectable signs of BBS. Although BBS patients are born with a birth weight within the normal range, by the age of 3 years old, 33% of BBS patients are obese and over time that statistic increases to 72-92% of BBS patients. A high frequency of genital anomalies is seen among BBS patients, ranging from hypogenitalism and infertility in males to abnormal genitalia in females. Although BBS patients are typically infertile, they are capable of reproduction. Another tell-tale sign of BBS is renal anomalies, a major cause of mortality among BBS patients; renal complications typically involve kidney malformation, cystic tubular disease, and urine concentration defects. Finally, BBS patients have significant difficulties with learning, including developmental delay and cognitive impairments as well as behavior abnormalities (Forsythe, et al., 2013).

Due to the disease's pleiotropic nature and the lack of any targeted BBS treatments, BBS must be treated on a case-by-case basis (Sheffield, 2010). Patients are encouraged to have several annual examinations to watch for potential complications including hypertension, diabetes mellitus, and obesity. Patients are also recommended to be genetically confirmed for BBS; oral glucose tolerance tests, speech therapy, consultation with a cardiologist, review by a clinical psychologist, and orthodontic and dentist work are recommended as needed based on phenotype (Sheffield, 2010).

Although the link between BBS and obesity and diabetes is not currently understood, it is widely believed that further research of BBS will reveal biochemical and

developmental pathways connected to the disease's phenotypic manifestations. The study of BBS and other rare diseases has already led to a better understanding of biology and the discovery of previously unidentified disease genes such as the *bbs* genes (Sheffield, 2010).

BBS Genes

Currently 16 BBS genes have been identified (Forsythe, et al., 2013; Mockel, et al., 2011). These genes, listed in **Table 2**, serve various functions within the cell, but they all relate to cilia function. Of the identified bbs proteins, seven form a complex known as the BBSome (BBS1, BBS2, BBS4, BBS5, BBS7, BBS8, and BBS9), three form a BBS chaperone complex (BBS6, BBS10, BBS12), and the other six are involved in cilia function (Sheffield, 2010).

Table 2: List of identified BBS genes (and other names) and their function (Forsythe, et al., 2013).

Gene	Locus	Function
BBS1	11q13	BBSome protein
BBS2	16q21	BBSome protein
BBS3 (ARL6)	3p12-p13	ADP-ribosylation factor-like small GTPase
BBS4	15q22.3-23	BBSome protein
BBS5	2q31	BBSome protein
BBS6 (MKKS)	20p12	Part of BBS chaperonin complex
BBS7	4q27	BBSome protein
BBS8 (TTC8)	14q32.1	BBSome protein
BBS9 (B1)	7p14	BBSome protein
BBS10	12q21.2	Part of BBS chaperonin complex
BBS11 (TRIM32)	9q31-q34.1	E3 ubiquitin ligase
BBS12	4q27	Part of BBS chaperonin complex
BBS13 (MKS1)	17q23	Centriole migration protein
BBS14 (CEP290)	12q21.3	Basal body: RPGR interaction protein
BBS15 (WDPCP)	2p15	Localization of septins and ciliogenesis protein
BBS16 (SDCCAG8)	1q43	Basal body: OFD1 interaction protein

The BBSome

The BBSome is a protein complex involved in the biogenesis of primary cilia. The BBSome is made up of BBS1, BBS2, BBS4, BBS5, BBS7, BBS8, and BBS9, and it is a highly conserved complex found in all ciliated organisms (Jin, et al., 2009). The BBSome has been related to intraflagellar transport (IFT) coordination and function, trafficking of signaling receptors to the primary cilium, IFT particle assembly at the ciliary base and ciliary tip, signaling interpretation of several hormones including leptin, ciliary membrane elongation, and regulation of dense-core vesicle secretion (Jin, et al., 2009; Seo, et al., 2010; Sheffield, 2010; Wei, et al., 2012; Zhang, et al., 2011; Lee, et al., 2011).

BBS1, one of the BBS proteins that make up the BBSome, has been shown to interact with leptin receptors (Seo, et al., 2010). Leptin is an adipocyte hormone involved in body weight regulation, and its recently discovered connection to BBS1 has led to a working hypothesis that BBS1 and the BBSome are involved in interpreting leptin signal. Leptin is a hormone used to indicate to the brain whether or not an organism has enough stored fat or if food intake should be increased, and disrupted leptin signaling has been related to obesity and high body weights, as seen in BBS patients (Jin, et al., 2009; Friedman, 2008) and animals. It is known that BBS knockout animals raised with strict dietary control in metabolic cages do not become obese (Guo, et al., 2011).

In addition to its role in leptin signaling, the BBSome regulates the movement of proteins and vesicles to the primary cilia, and it has been indicated as an important player in IFT. The main role of the BBSome in this capacity is to efficiently assemble IFT particles and reorganize the IFT complex at the base of the cilia and again at the ciliary tip to promote anterograde and retrograde transport respectively (Wei, et al., 2012).

Although IFT can take place in the absence of the BBSome, studies show this leads to lowered IFT coordination and disrupted retrograde transport (Jin, et al., 2009; Wei, et al., 2012). A schematic drawing of the BBSome and an illustration of its role in IFT are shown in **Figure 3**.

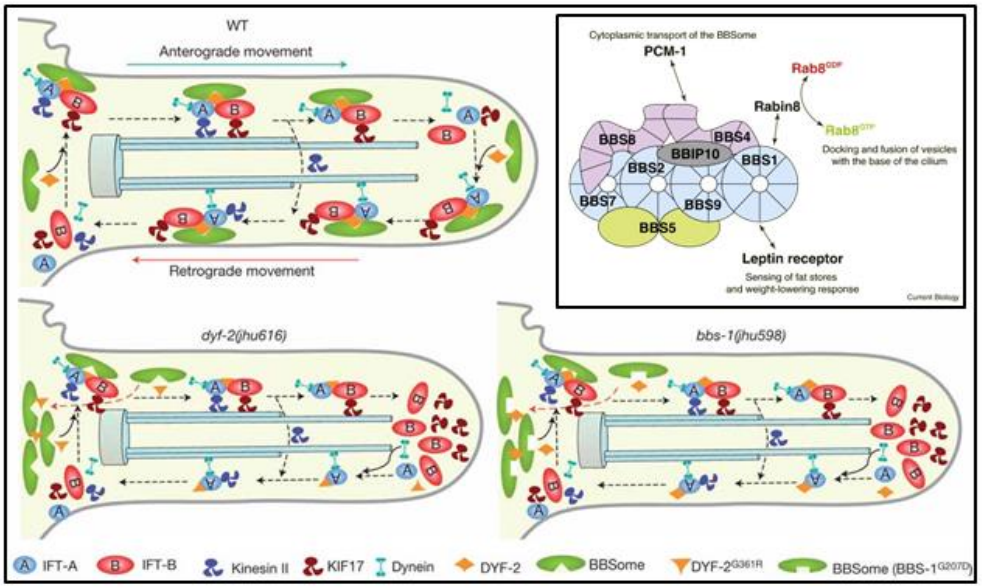

Figure 3: A schematic drawing of the BBSome complex with molecular interactions (Jin, et al., 2009) and a model for the BBSome's role in IFT assembly and turnaround adapted from (Wei, et al., 2012).

BBS Chaperonin Complex

The BBSome is assembled by a chaperonin complex made of BBS6, BBS10, and BBS12. These chaperonin proteins, which are only found in vertebrates, rather than in all ciliated organisms, interact with chaperonin containing TCP-1 (CCT) proteins to mediate assembly of the BBSome by forming a multisubunit complex (Seo, et al., 2010). The BBS chaperonin proteins associate with BBS7 during BBSome assembly, and together these proteins assist with the folding of BBSome subunits and BBSome subunit assembly to create the BBSome complex. The three BBS proteins allow CCT proteins to interact

with the BBSome to perform protein folding; however, the BBS proteins don't appear to actively participate in protein folding themselves (Seo, et al., 2010).

Additional BBS Genes

In addition to the BBSome and BBS chaperonin complex proteins, there are six other BBS proteins. BBS3 is also known as ADP-ribosylation factor-like small GTPase (ARL6). While BBS3 is predominantly involved in moving the BBSome to the cell membrane, it has also been shown to interact with Golgi vesicles and plasma membrane which later become ciliary membrane. Although the *in vivo* function of BBS3 is not yet fully understood, it has been shown to have a role in mediating K_v and K_{Ca} channels (Valentine, et al., 2012). Recently, tripartite-motif-containing protein 32 (TRIM32) has been shown to be BBS11. BBS11 is a widely expressed degradation compound that regulates dysbindin (Locke, et al., 2009; Chiang, et al., 2006). BBS13, also called Meckel-Gruber Syndrome 1 gene (MKS1) is involved in ciliogenesis, and mutations in BBS13 have been shown to disrupt Wnt and Shh signaling (Wheway, et al., 2012; Valentine, et al., 2012). The BBS14 protein is known as both CEP290 and NPHP6. BBS14 localizes to cilia, centrosomes, and nuclei, where it plays an important role in chromosome separation. Mutations in BBS14 have led to disrupted intraciliary and axonal transport, indicating a role for BBS14 in IFT (Frank, et al., 2008). BBS15 is believed to be WD repeat containing planar cell polarity effector (WDPCP), a tissue-specific planar cell polarity effector gene which may control primary cilia formation and function (Mockel, et al., 2011; Dai, et al., 2013). The BBS16 protein is SDCCAG8, a part of photoreceptor sensory cilium proteome and human centrosomal proteome. While BBS16 depletion leads to kidney cysts, body axis defects, and cell polarity defects, all of

which are seen in ciliopathies, the precise relation between BBS16 and cilia function remains to be discovered (Otto, et al., 2010).

Effect of Primary Cilia on Cell Cycle

The cell cycle is composed of four main stages: G1, S, G2, and M (**Figure-4**). G1 is the first of the two gap phases, and it allows the cell to determine whether or not environmental conditions are conducive to cell growth and division (Alberts, et al., 2002). After G1 the cell transitions to the S (synthesis) phase, in which the cell replicates its DNA. The cell then spends a small amount of time in G2, the second gap phase, before it moves into M (mitosis), during which time cell division occurs. If conditions are unfavorable for cell division, however, the cell can enter G0, a prolonged resting phase in which cells can remain for an extended amount of time (Alberts, et al., 2002).

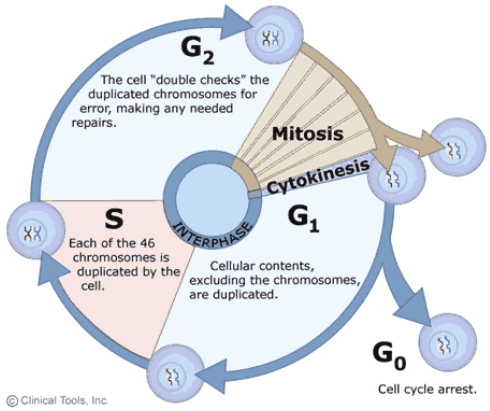

Figure 4: Schematic drawing of cell cycle progression (2010).

Recently it has been observed that upon entering the cell cycle, most cells disassemble their primary cilia; then, upon cell cycle completion, primary cilia are reassembled (Goto, et al., 2013; Quarmby, et al., 2005). Although it is not currently known whether or not ciliogenesis and progression through the cell cycle are mutually exclusive events, it has been shown to be a possibility (Goto, et al., 2013). Additionally,

research has shown that forced suppression or induction of ciliogenesis affects cell cycle progression, and it especially affects the transition from G0 to G1, supporting the idea that the presence or absence of primary cilia play a role in cell cycle progression (Goto, et al., 2013).

Wnt Signaling Pathway

Members of the wingless-type MMTV integration site family (wnt) are a group of secreted glycoproteins involved in tissue remodeling and homeostasis (Christodoulides, et al., 2009). In vivo, *wnt* signaling represses adipogenesis, as proven when disrupted wnt/β-catenin signaling induced adipogenesis (**Figure-5**). Additionally, wnt/β-catenin functioned during early development to prevent mesenchymal precursors from differentiating into adipocytes, further supporting a role for *wnt* signaling as an adipogenesis preventer (Christodoulides, et al., 2009). The *wnt* signaling pathway is composed of two individual pathways, the canonical and non-canonical *wnt* pathways.

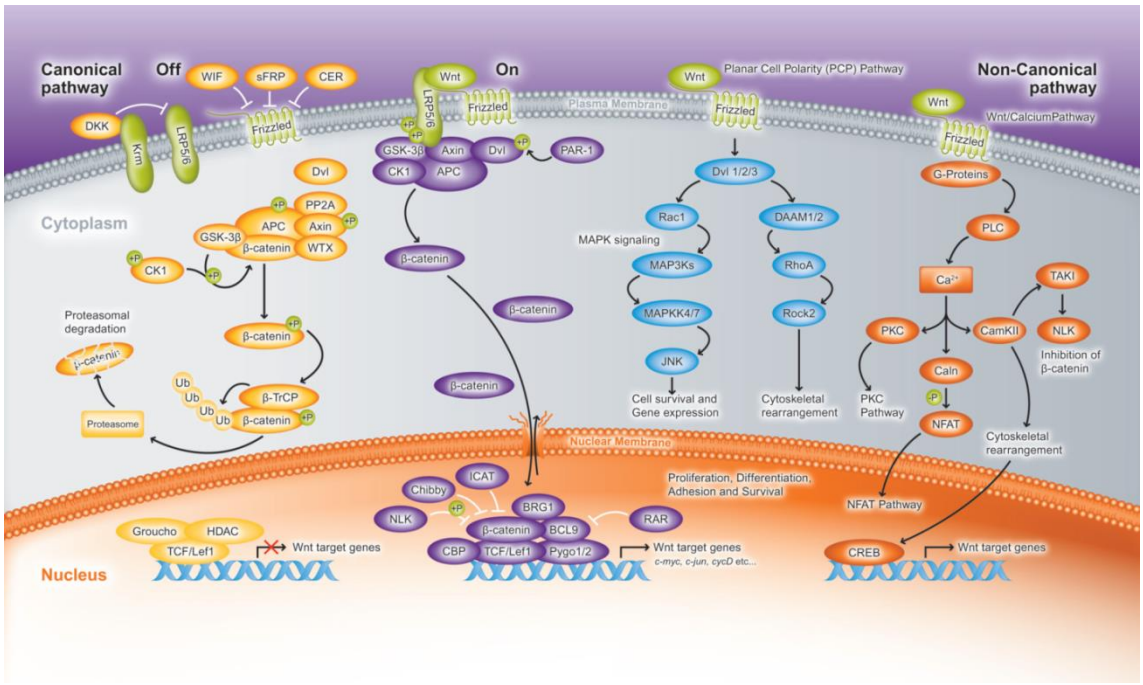

Figure 5: The canonical wnt signaling pathway, planar cell polarity pathway, and non-canonical wnt signaling pathway showing proteins and target genes involved in *wnt* signaling (Abcam, 2012).

The canonical *wnt* signaling pathway regulates β-catenin by binding to frizzled (Frz) and lipoprotein-related-receptor-protein 5 or 6 (LRP 5/6) to inactivate the degradation complex that β-catenin forms (Christodoulides, et al., 2009). Although not yet fully understood, the non-canonical *wnt* signaling pathway works antagonistically to the canonical *wnt* pathway. It is believed that the non-canonical *wnt* signaling pathway might be regulated by ciliary function since it promotes adipogenesis (Christodoulides, et al., 2009).

PROJECT PURPOSE

The specific link between Bardet-Biedl Syndrome and the development of obesity and type II diabetes among BBS patients is not currently understood. However, it is widely believed that further research of BBS will reveal biochemical and developmental pathways instrumental in understanding the disease's physical manifestations. This project examined how loss of the Bardet-Biedl Syndrome 2 gene affected the pancreas, glucose tolerance, and insulin sensitivity in order to gain a clearer understanding of how BBS causes obesity and type II diabetes. Only by understanding how these diseases develop can they one day be cured and prevented.

METHODS

Ethics Statement

All animals were housed in a viral-antibody-free facility and maintained according to both the *Guide for the Care and Use of Laboratory Animals* (Institute of Laboratory Animal Resources, 1996) and the University of Massachusetts Institutional Animal Care and Use Committee (IACUC). All animal-related research was approved by the University of Massachusetts IACUC.

Cell Culture

Rat insulinoma (INS1) cells were a gift from Dr. Fumihiko Urano at the University of Massachusetts Medical School. Insulinoma cells were grown in RPM1 1640 media (Gibco, California) and supplemented with 10% fetal bovine serum (FBS), penicillin and streptomycin and concentrated sodium pyruvate A and BME. Cell cultures were kept at 37°C in an atmosphere of 5% CO_2. The medium was changed every 3-4 days and cells were regularly passaged twice a week.

siRNA Transfection

The siRNA used were from Ambion (California): siBBS2 5' AAUAUCAUCAGUAUUCACCgt and scrambled (SCR, control) 5' CAGUCGCGUUUGCGACUGG. Cells that siRNA transfection was performed on were plated in 6-well plates at 800,000 cells/well. Transfection with 10µL of siRNA was performed according to the manufacturer's protocol using the lipofectamine 2000 reagent from Invitrogen. The optimal siRNA concentration was determined by using concentrations of 5µL and 10µL of siRNA. Since 10µL of siRNA after a 72 hour

transfection gave the most efficient knockdown, all subsequent experiments were performed using 10μL of siRNA for 72 hours.

Western Blotting

Insulinoma cells or pancreatic islets were prepared for western blot analysis by following the Pierce NE-PER Nuclear and Cytoplasmic Extraction Reagents lysate protocol using the cytosolic and nuclear lysate buffer from Pierce (Illinois). Denatured lysates were run on a Novex® 4-20% gradient gel with 1.5mm x 10 wells (Life Technologies, Massachusetts). Prior to loading, the concentration of lysates loaded into the gel were determined according to the Thermo Scientific Pierce 600nm Protein Assay from Pierce (Illinois). After the gels were run and transferred for 2 hours at 100mV to PVDF membranes, the membranes were blotted in 5% blotting-grade blocker nonfat dry milk from Bio Rad (Massachusetts) in Tris-Buffered Saline with 0.05% Tween 20 (TBST) for 1 hour at room temperature. Primary antibodies were applied overnight in 5% milk. The primary antibodies used include BBS2 (Abcam, Massachusetts); Insulin (Sigma Aldrich, Massachusetts); Total β-catenin (Abcam, Massachusetts); P9 GSK3β (Cell Signaling Technology, Massachusetts); Cyclin D1 (Cell Signaling Technology, Massachusetts); LRP 5/6 (Novus Biologicals, Colorado); and Active β-catenin (Millipore, Massachusetts). Secondary antibodies were applied for 1 hour at room temperature in 5% milk TBST. The secondary antibodies used include goat anti-mouse or goat anti-rabbit HRP (Dako, California) conjugated at concentrations of 1:5,000 and 1:3,000 respectively. The loading control used was actin from Millipore. The film was developed using HRP developing solution from GE Healthcare (Massachusetts), and luminescence was quantified using Adobe Photoshop software. Quantification was

performed by placing a box around the band and multiplying the average intensity by the area. This number was then calculated as a percent of the average intensity and area of the actin loading control.

FACS/Cell Cycle Analysis

Two wells from 72 hour, 10µL siRNA transfected insulinoma cells cultured at 800,000 cells/well were combined. The cells were lifted with trypsin EDTA solution and made into a single cell suspension before the cells were pelleted and fixed drop-wise in 500µL of -20°C 100% ethanol. SCR and siBBS2 cells were FACS sorted and cell cycle analysis was performed using MODFIT analysis by the University of Massachusetts Core Facility.

Mouse Model

The BBS2 mice used were a gift from Dr. Val C. Sheffield from Iowa, MD. Eight- to 15-week old mice of either sex were used. Mouse pancreatic islets were harvested according to (Parker, et al., 1995). A BBS2 genotyping test consisting of 4 specific primers mixed equally was used to determine each mouse's genotype. The ~600bp band indicates wild type while the ~350bp band indicates a knock-out BBS2 mouse. In Figure 6 below BBS2 mice genotyping is shown.

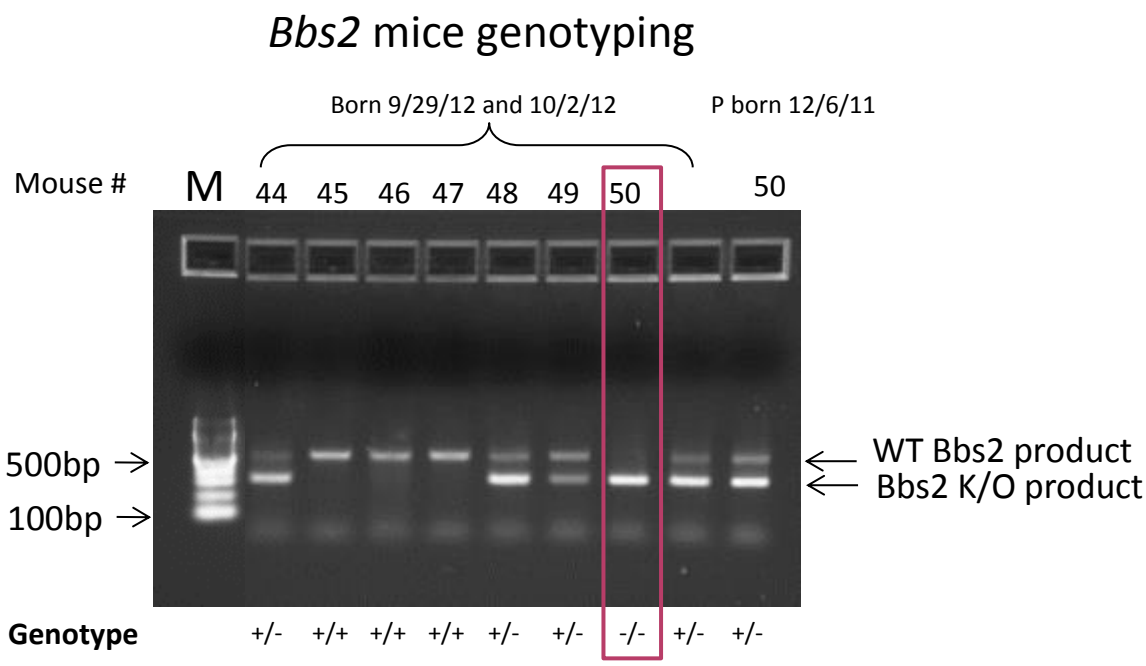

Figure 6: BBS2 Mice Genotyping

Immunofluorescence

Islets were fixed in 3.7% paraformaldehyde for 30 minutes at room temperature, and immunofluorescence was performed as described by (Gromley, et al., 2005). The primary antibodies included: BBS2 (1:100) (Abcam, Massachusetts); Insulin (1:250) (Sigma Aldrich, Massachusetts); Pericentrin (BD Biosceinces, California); and Acetylated Tubulin (1:100) (Abcam, Massachusetts). The secondary antibodies were Alexa-Fluor antibodies used at a concentration of 1:1,000; Cy-5 was used at a concentration of 1:100; and DAPI was used at a concentration of 1:10,000 (Sigma-Aldrich). Coverslips were mounted with Prolong Antifade medium (Invitrogen). Images were taken using spinning-disk confocal microscopy on a Nikon Eclipse TE2000-E microscope, deconvolved, and analyzed using NIS Elements Analysis software.

Fluorescence intensity was determined by drawing a box around a specific area and the average intensity per pixel was recorded.

Glucose Tolerance Test

Blood glucose levels were determined by using an Accu-Check Active meter (Roche Diagnostics, Indiana) which tested a blood sample taken via a tail bleed. The day before the glucose tolerance test, a pre-fast (nonfasting) blood glucose and body weight were recorded. The animals were fasted overnight, and body weight and blood glucose readings were taken at timepoint 0. The insulin used was dissolved in 5mL of phosphate buffered saline (PBS) for every 1 gram of glucose, and mice were given an intraperitoneal injection of 2 grams of glucose for every kg of body weight. Blood glucose was recorded at 15, 30, 60, 90, and 120 minutes post glucose injection.

Insulin Tolerance Test

As described above, blood glucose levels were determined by using an Accu-Check Active meter (Roche Diagnostics, Indiana). Prior to insulin tolerance testing (ITT) the animals were fasted for 5 hours and then the ITT was performed by challenging mice with 3 times their body weight of 0.20units/mL of humulin insulin diluted in sterile saline. Blood glucose levels were recorded at time points 0, 15, 30, 60, 90, and 120 minutes post-injection.

Perifusion

A perifusion was performed on mouse islet cells that were isolated and plated overnight at 37°C. The following day the islets were counted and 25-50 islets were placed into an islet perifusion chamber using the islet perifusion instrument from National Instruments, Inc. (Florida). Islets were stimulated with a basal solution of

2.5mM glucose for 90 minutes at a rate of 90 reps/1 minute per rep/100µL/minute. The basal solution was removed and the cells were placed in the glucose stimulation solution of 20mM glucose for 35 minutes at 35 reps/1 minute per rep/100µL/minute, after which time the islets were again stimulated in basal solution for 15 minutes at a rate of 15 reps/1 minute per rep/100µL/minute. The islets were then stimulated in the second glucose stimulation, a 20mM glucose solution, for 35 minutes at 35 reps/1 minute per rep/100µL/minute. After this time the islets were subjected to KCl stimulation in a solution of 20mM KCl for 10 minutes at 10 reps/1 minute per rep/100µL/minute. The solution was removed and replaced with the basal solution for 15 minutes at 15 reps/1 minute per rep/100µL/minute. A total insulin extraction was then performed in 1mL of acidified ethanol extracted overnight at -20°C.

Cilia Counts and Length Measurements

Islets stained for pericentrin (centrosome marker), acetylated tubulin (cilia marker), and insulin were imaged using a 40X Plan/Apo lens on a Solamere Technology Group CSU10B Spinning Disk Confocal Microscope (Digital Light Microscopy Core, University of Massachusetts Medical School). A z-series of 50µm thick images were taken for each islet and used for cilia length measurements. The polyline length analysis feature of NIS Elements Analysis software was used to trace a line over the length of a cilium. The software then measured the length in pixels of the line that was drawn. Cilia lengths were recorded and converted to µm. Cilia were categorized by length as either short (< 8.00µm), medium (≥ 8.00µm and < 20.00µm), or long (≥ 20.00µm) so that statistical analysis of cilia lengths could be performed.

Statistics

Statistical analysis was performed using Microsoft Excel. Differences were compared using two-tailed unimpaired t-tests. Values of $p < 0.05$ were considered statistically significant *, $p < 0.01$ was **, and $p < 0.001$ was ***.

RESULTS

The high frequency of obesity and type II diabetes among Bardet-Biedl Syndrome patients has brought attention to the syndrome as a way to discover biochemical and developmental pathways involved in the development of these diseases in BBS patients. Hopefully a clearer understanding of how obesity and type II diabetes arise in BBS patients will one day lead to the ability to prevent and cure these diseases. Since obesity and type II diabetes are known to be related to pancreatic function and insulin, this project looked at how knockout of the Bardet-Biedl Syndrome 2 gene affected the pancreatic islets' morphology, glucose tolerance, and insulin sensitivity. BBS2 knockdown resulted in low insulin levels in mice and glucose intolerance; however, the knockdowns had normal insulin sensitivity compared to the wild type. The primary cilia of BBS2 knockouts showed a distinct phenotypic difference where they were fewer, shorter, and less organized than in the wild type. *In vitro* knockdown of BBS2 led to lower insulin levels and downregulation of several canonical *wnt* signaling proteins, including Cyclin D1, a cell cycle progression marker. FACS cell cycle analysis of BBS2 knockdown cultures showed disrupted cell cycle due to s-phase arrest.

BBS2 Knockout Mice Are Born Small

The BBS2 knockout mouse model used was a gift from Dr. Val C. Sheffield. Mice were genotyped to determine if they were wild type (WT), BBS2 heterozygous (BBS2 Het), or BBS2 negative homozygotes (BBS2 KO). The BBS2 KOs were born abnormally small compared to their WT littermates (**Figure 7**). The KO mice showed a distinct BBS2 phenotype while the heterozygotes didn't appear to have any specific phenotype.

Figure 7: A BBS2 knockout mouse model. An image of the mice pups at a few days old, emphasizing the atypically small size of the BBS2 KO mice (left) compared to their WT litter mate (right).

In vivo analysis was performed using mice from the BBS2 mouse model in Figure 7. The glucose tolerance test (GTT), insulin tolerance test (ITT), and perifusion tests were all performed using an n of 2 animals.

BBS2 Knockout Mice are Glucose Intolerant and Have Lower Insulin Levels

A glucose tolerance test was performed on WT, BBS2 Het, and BBS2 KO mice. Blood glucose levels were taken from the mice at various time points throughout the test, starting with a steady state, pre-fasting blood glucose reading. The mice were fasted overnight, after which time the time 0 blood glucose reading was taken. The mice were then injected with glucose, and blood glucose readings were taken at 15, 30, 60, 90, and 120min after injection.

For the first 30 minutes a spike in blood glucose levels occurred as expected (**Figure 8A**). After this time, the body typically releases enough insulin to begin absorbing glucose into the surrounding tissue and a drop in blood sugar is seen. Blood

sugar levels are expected to continue to drop until they reach normal. The results of the GTT are shown along with plasma insulin readings taken pre-fasting and at time 0 min (**Figure 8B**).

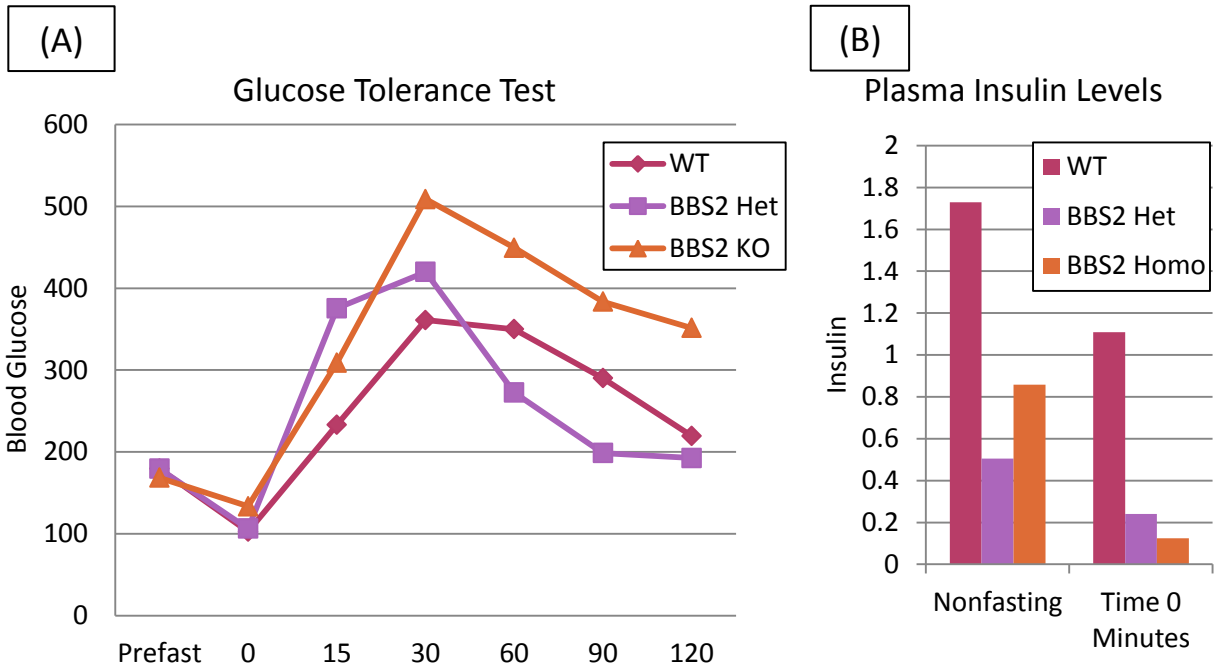

Figure 8: Glucose tolerance test (GTT) shows glucose intolerance in BS2 knockout mice. (A) In the GTT, BBS2 KO mice had elevated blood glucose levels compared to WT mice, and they remained elevated for the duration of the test. Persistent high blood glucose levels implies that the KO's are either unable to produce enough insulin in response to the glucose or their cells are not properly responding to insulin. (B) Insulin levels in the plasma were measured at two time points during the GTT. The Hets and KOs had lower nonfasting and time 0 insulin levels than the WT.

In the GTT, the BBS2 KO mice experienced a much higher and steeper spike in blood glucose levels. While the BBS2 KOs eventually showed decreased blood sugar levels, they were never able to come down as far or as fast as the WT or BBS2 Hets (Figure 8A). It was interesting to note that at the final time point, 120 minutes after the glucose injection, the BBS2 KO mice's blood sugar levels started decreasing more slowly even though they were still significantly above 300 mg/dL. In addition to blood glucose levels, plasma insulin levels were measured pre-fast and at 0 min (Figure 8B) and show that both the BBS2 Hets and BBS2 KOs have much lower insulin levels than the WT.

From this it is apparent that BBS2 KO mice are glucose intolerant since they are unable to remove glucose from the blood stream as efficiently or as quickly as the WT were able to. Typically glucose intolerant animals compensate for this by producing more insulin; however, the BBS2 KOs have unusually low insulin levels, so they are unable to compensate for their glucose intolerance.

BBS2 Knockout Mice are Insulin Resistant

An insulin tolerance test (ITT) was performed on the mice to determine their insulin sensitivity and their ability to remove insulin from the blood stream (**Figure 9**). Mice were injected with insulin and their blood glucose levels were monitored 15, 30, 60, 90, and 120 minutes after injection.

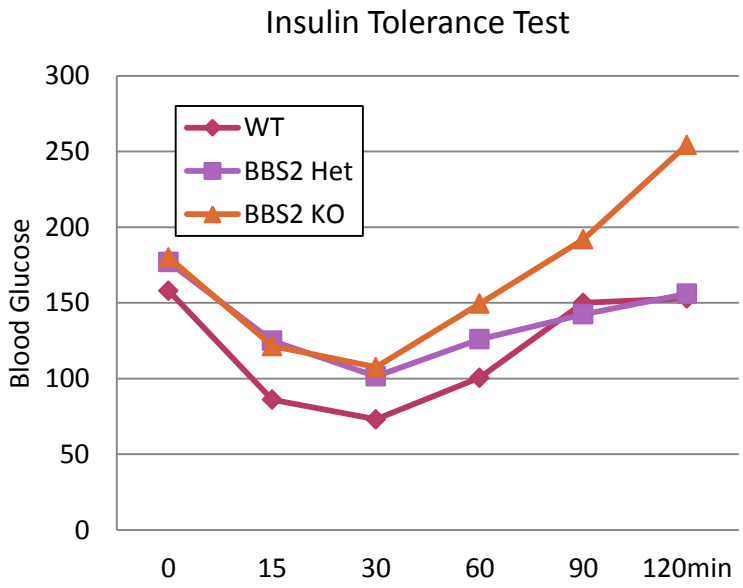

Figure 9: BBS2 Hets and BBS2 KOs are insulin sensitive. This indicates that the results seen in the GTT are due to insulin resistance.

The WT, BBS2 Hets, and BBS2 KOs all appeared to be equally insulin sensitive (Figure 9). As expected, all three experienced decreased blood sugar levels over the first half hour. Although the BBS2 Het and the BBS2 KO had higher blood sugar levels than

the WT, their blood sugar levels all decreased at the same rate, indicating equal insulin sensitivity. After the half hour timepoint, all animals' blood sugar levels began increasing, indicating that they were able to absorb the excess insulin into the liver and the muscles to prevent hypoglycemia. At this point blood sugar levels rose to a normal level before they plateaued at a steady state. This was not seen among the BBS2 KO mice whose blood sugar levels did not plateau and instead rose to 250 mg/dL, indicating that BBS2 KOs are insulin resistant.

Knockout of BBS2 Decreases Insulin Levels in Pancreatic Islets

In order to see how BBS2 knockout affects pancreatic insulin levels, sections of pancreas were mounted onto slides and stained for BBS2 and insulin (**Figure 10A**). An epifluorescent microscope was used to observe the pancreatic islets. BBS2 Hets (n = 40) were used as controls for the BBS2 KOs (n = 21). Quantitization was performed by measuring the intensity of the BBS2 or insulin staining (Figure 10B) using NIS Elements Analysis software.

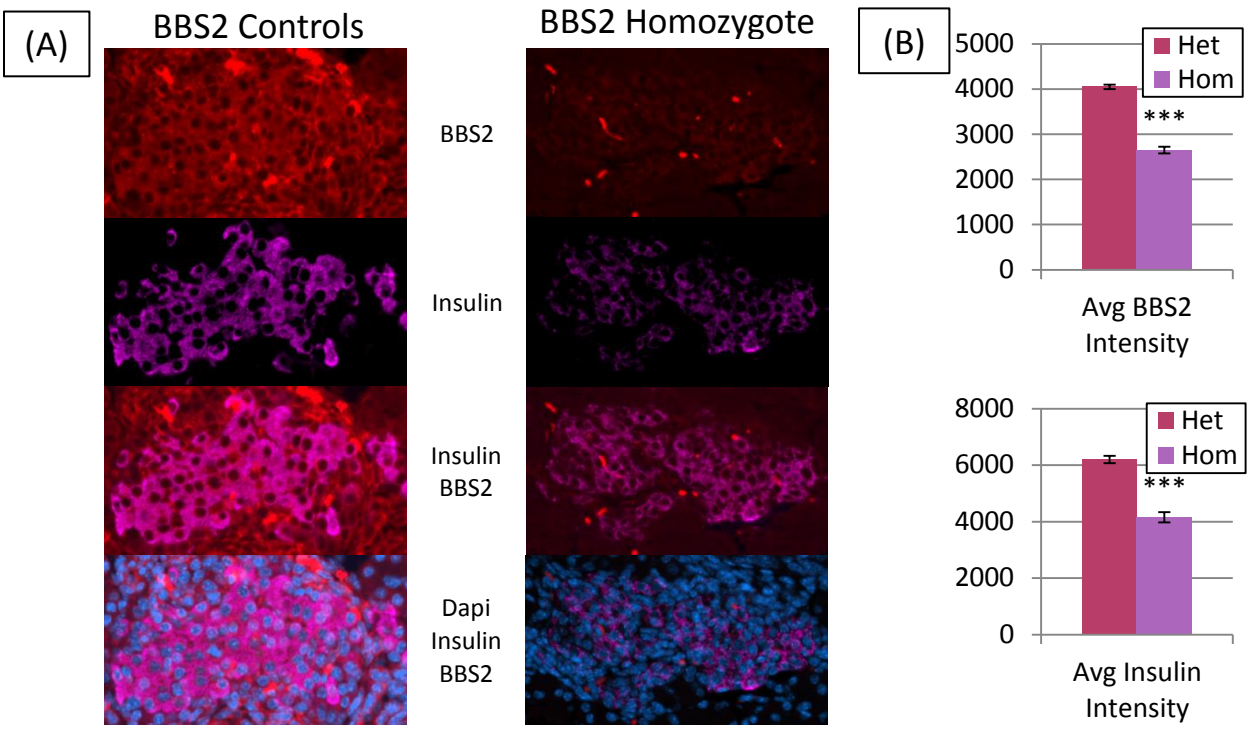

Figure 10: BBS2 knockout decreases insulin levels in pancreatic islets. (A) Pancreatic tissue from a heterozygous BBS2 mouse and a BBS2 KO mouse was stained for BBS2 (red), insulin (purple), and overlaid with DAPI (blue). Comparison shows lower BBS2 and insulin levels in the KO mouse compared to the heterozygote. (B) BBS2 and insulin intensities were compared between the heterozygote and BBS2 KO, and lower levels of BBS2 and insulin in pancreatic islets was observed.

The staining showed that BBS2 (**Figure 10A**, top) is a cytosolic protein expressed in the pancreas, and while it is present in islets, BBS2 is not exclusively expressed there as it is also expressed in insulin negative cells. Using NIS Elements software, the intensity of the BBS2 staining was quantitized, showing significantly reduced levels of BBS2 (**Figure 10B**, top). Similarly, insulin levels were determined, and analysis showed significant knockdown of insulin in BBS2 KO islets compared to the controls (Figure 10B, bottom). From these stains it is apparent that BBS2 knockout leads to decreased insulin levels in pancreatic islets.

BBS2 Knockout Shows Abrogated Insulin Secretion

Since insulin levels are difficult to determine *in vivo* due to compensatory mechanisms to keep the glucose level in check, pancreatic islets from WT, BBS2 Hets,

and BBS2 KOs were isolated and cultured overnight so that insulin secretion in the islets could be determined *in vitro*. This was accomplished by performing a perifusion test (**Figure 11**). Plated islets were treated with various stimulatory solutions and the amount of insulin secreted by the islets was measured.

First the islets were treated with a non-stimulatory basal solution that was 2.5mM glucose; they were then stimulated with a 20mM glucose solution. Next the non-stimulatory 2.5mM glucose solution was used to returned the cells to normal insulin secretion, and after this they were again stimulated with a 20mM glucose solution. Finally, the islets were then treated with a 20mM KCl solution which depolarized the islets' cell membranes, opening Ca^{+} channels, and allowing the islets to excrete all releasable insulin, about 1-2% of the total insulin contained in the islet. After this was done, the islets were again treated with 2.5mM glucose solution. Acidified ethanol was then used to lyse the islets' cell membranes and all of the insulin contained in the islets was released and could be measured.

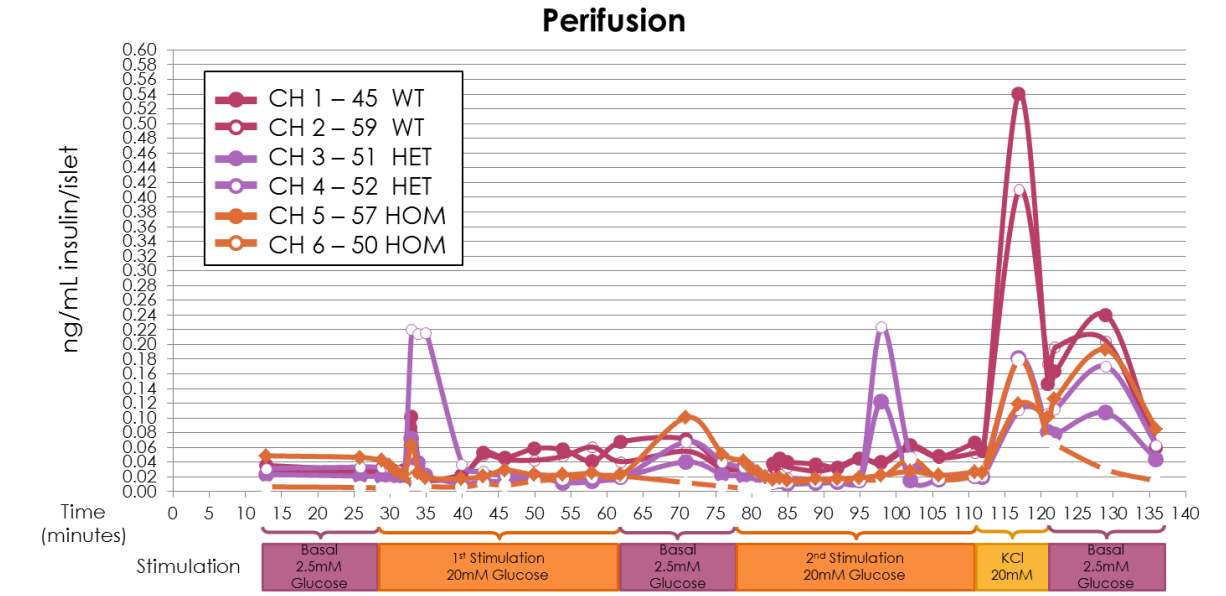

Intracellular insulin/islet (ng/mL)					
CH 1 (WT) = 101.18	CH 3 (Het) = 32.38	CH 5 (Hom) = 48.99
CH 2 (WT) = 92.87	CH 4 (Het) = 54.38	CH 6 (Hom) = 75.59

Figure 11: Despite low overall levels of insulin, BBS2 heterozygotes hypersecrete insulin in response to glucose stimulation while BBS2 KOs hyposecrete insulin. (A) Pancreatic islets were isolated and in vitro insulin levels were tested. Islets were stimulated in a series of solutions: 2.5mM glucose basal solution, 20mM stimulatory solution, and 20mM KCl. The 20mM glucose stimulation shows how islets respond to glucose. The KCl stimulation depolarizes the cell membrane, and the total releasable insulin in the islets was measured. BBS2 Hets hypersecrete insulin in response to glucose stimulation while BBS2 KOs hyposecrete insulin. Both Hets and KOs contain lower levels of releasable insulin than the WT. (B) After the perifusion was completed, acidified ethanol was used to lyse the islets so the total amount of insulin remaining in the islets could be determined. WT islets contained significantly more insulin than both the Hets and KOs, which have low total insulin levels.

When the islets were stimulated with the 20mM glucose solution, the BBS2 Hets responded by hypersecreting insulin but the BBS2 KOs hyposecreted insulin. This unexpected result shows that while knockout of BBS2 leads to insulin hyposecretion, knockout of just one copy of the BBS2 gene results in insulin hypersecretion in response to glucose stimulation. Despite the Hets ability to hypersecrete insulin, both they and the KOs contained much lower levels of releasable insulin than the WT islets. Additionally, the total insulin levels measured in the WT islets were 101.18 ng/mL and 92.87 ng/mL. These levels are higher than the total insulin levels in the BBS2 Hets (32.38 ng/mL and 54.38 ng/mL) and the BBS2 KOs (48.99 ng/mL and 75.59 ng/mL).

Primary Cilia in BBS2 Knockouts are Shorter and Fewer

Cross sections of pancreatic tissue from WT and BBS2 KO mice were collected and mounted on slides. Immunofluorescence was used to probe for pericentrin (**Figure** 12**A & H**), acetylated tubulin (**Figure** 12**B & I**), and insulin. Figure 12 shows WT and KO islets stained for various proteins. NIS Elements Analysis software was used to trace a line over the length of the cilia; the computer then determined how long the cilia were in pixels, and the length was converted to μm. Images were taken in a z-series to count the cilia, but are presented as maximum intensities across the z-series.

Figure 12: BBS2 mutation affects primary cilia morphology in pancreatic islet cells. Images of WT pancreatic islets (left) compared to KO islets (right) were taken using confocal microscopy to observe primary cilia presence and morphology. Staining shows pericentrin (green) and Dapi (A & H); acetylated tubulin (red) and Dapi (B & I); and pericentrin, acetylated tubulin, insulin (purple) and Dapi (C & J). A z-series of images were taken, and a maximum expose across the z-series was examined for pericentrin and acetylated tubulin (D & F). Pericentrin and acetylated tubulin staining were used to determine primary cilia lengths (E & G). Inlays show a magnified image of a primary cilium for both maximum intensity and cilia lengths. WT images (A-E) appear more organized, and they have a higher density of centrosomes and cilia compared to the BBS2 KOs (F-J).

Figure 12 shows overlays of pericentrin and Dapi (Panels A & H); acetylated tubulin and Dapi (Panels B & I); pericentrin, acetylated tubulin, insulin, and Dapi (Panels C & J); a maximum intensity exposure of pericentrin and acetylated tubulin (Panels D & F); and pericentrin and acetylated tubulin with cilia tracings (Panels E & G). Inlays show a single cilia attached to a centrosome (Panels D – G). The WT and BBS2 KO islet images show a distinct phenotypic difference between the two. The WT primary cilia appear more numerous and organized. The BBS2 KO islets appear to have few, poorly organized cilia that aggregated into indistinct clusters. Although the BBS2 KO cilia appeared to be shorter than the WT, cilia length measurements were collected and compared in **Figure 13**.

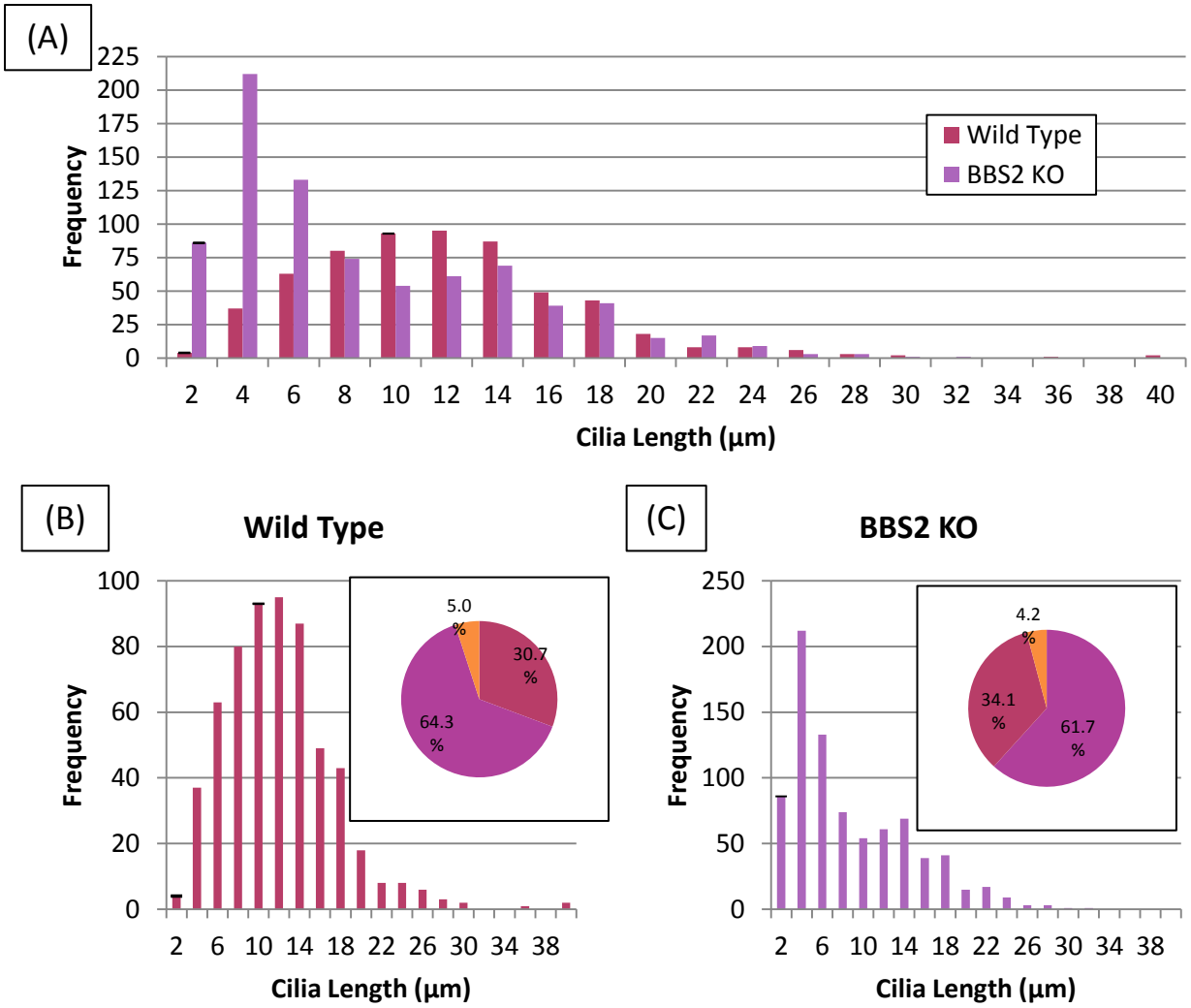

Figure 13: Primary cilia in pancreatic islets of BBS2 KOs are shorter than in the WT. (A) Cilia traced in pancreatic islets were measured and graphed as histograms. (B & C) Primary cilia lengths were categorized as either short (< 8.00 µm), medium (8.00 µm - 20.00 µm), or long (> 20.01µm). The percent of total cilia in each category was determined in WT and BBS2 KOs, and is represented in pie charts (inlaid). Cilia lengths in WT islets were 64.3% medium, 30.7% short, and 5.0% long (B). BBS2 KO islets contained 61.7% short cilia, 34.1% medium, and 4.2% long (C).

The histograms of cilia lengths show the number of cilia counted in increments of 2µm. There is clearly a distinct phenotypic difference between WT (n = 599) and BBS2 KO (n = 818) cilia. A comparison of the lengths (Figure 13A) shows that while the WT cilia tend to be medium length with some short and long cilia, the BBS2 KO cilia were generally short with some medium and long cilia. Inlaid in Figure 13B & C are pie charts showing the percent of total cilia counted that belonged to WT and BBS2 KO islets

respectively. The WT had 30.7% short cilia, 64.3% medium cilia, and 5.0% long cilia. The BBS2 KO had 61.7% short cilia, 34.1% medium cilia, and 4.2% long cilia. It is surprising that despite the marked difference in the percent of short vs. medium cilia between the WT and BBS2 KO, they had similar percentages of long cilia.

BBS2 Knockdown Results in Decreased Insulin Levels

BBS2 was knocked down *in vitro* using a rat insulinoma cell line. Lipofectamine was used to transfect the cells with 10μL of siRNA against BBS2 or scrambled (SCR) siRNA. Seventy-two hours after transfection, the cells were lysed and cytosolic extract was collected. Western blot analysis was performed on the denatured lysates and insulin was probed for (**Figure 14, top**); actin was used as a loading control. Quantitization was performed on the western by drawing a perimeter around the band that was presented. The average intensity of the band was multiplied by the area of the band and normalized to actin (**Figure 14, bottom**). Statistical analysis was performed on insulin intensity levels between the SCR and siBBS2 lysates.

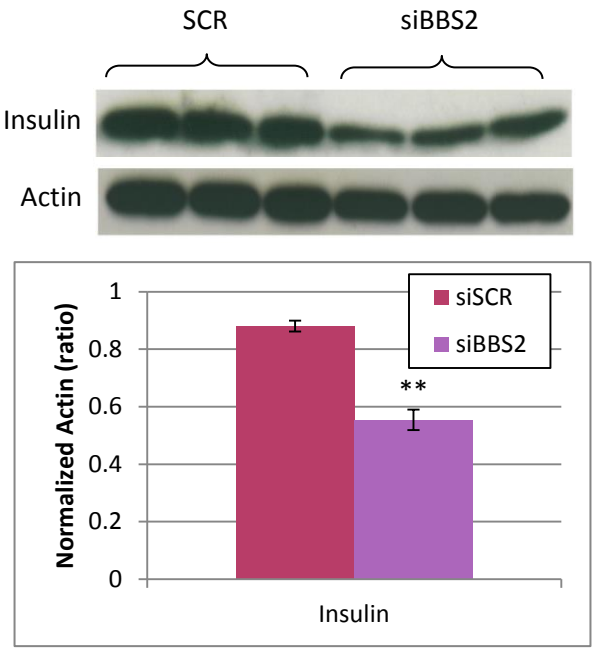

Figure 14: Lower insulin levels induced by BBS2 knockdown. Knockdown of BBS2 was accomplished in vitro using siRNA against BBS2; SCR siRNA was used as a control. A western blot analysis was performed to compare insulin levels between the SCR and siBBS2 and shows significantly lower levels of insulin in siBBS2 cells compared to the control.

BBS2 knockdown resulted in lower insulin levels among insulinoma cells compared to those transfected with SCR siRNA. Although insulin levels were visually lower in the siBBS2 cells, quantitization showed significant reduction of insulin between the siBBS2 and control.

Downregulation of *wnt* Signaling Genes in BBS2 Knockdown

BBS2 knockdown was most completely achieved by transfecting cells with siRNA and collecting lysates 72 hours after transfection. One western, however, was run with 5µL and 10µL of siBBS2 to determine which concentration was more effective at knocking down BBS2. Figure 15 shows that BBS2 knockdown was most effective when 10µL of siBBS2 were used, so all remaining siRNA transfections were performed with 10µL of siBBS2.

In addition to observing how BBS2 knockdown affected insulin levels, various genes involved in the canonical *wnt* signaling pathway were probed for (**Figure 15**). BBS2 was probed for to ensure that siRNA knockdown of BBS2 was successful.

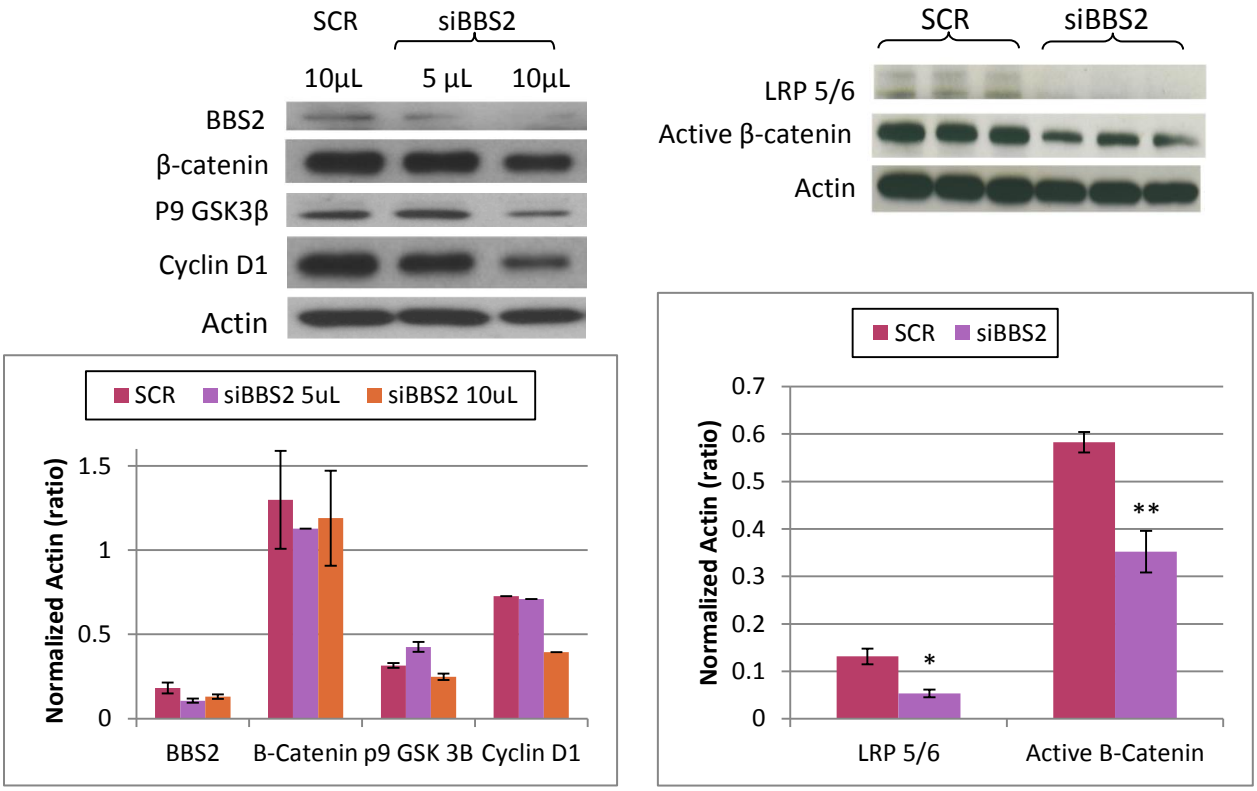

Figure 15: BBS2 knockdown results in downregulation of canonical wnt signaling proteins. Western blot analysis of cytosolic lysates from 72 hour siRNA knockdowns were probed for various proteins involved in the canonical wnt signaling pathway. BBS2, total β-catenin, P9 GSK3β, Cyclin D1, LRP 5/6, and active β-catenin were all downregulated in BBS2 knockdown.

The canonical *wnt* signaling pathway is involved in adipogenesis repression. Due to the high prevalence of obesity and diabetes mellitus among BBS patients, it was expected that canonical *wnt* signaling would be disrupted as a result of BBS2 knockdown. Total β-catenin is a cytosolic protein which forms a degradation complex if it isn't activated by the *wnt* signaling pathway. BBS2 knockdown led to slightly lower levels of total β-catenin; however, while there was a slight difference it does not appear to be significant. Phospho-9-GSK3β (P9GSK3β) is an inhibitory phosphorylation of GSK3β

which leads to inactivation of this constitutively active protein and turns on *wnt* signaling. This leads to accumulation of β-catenin and translocation to the nucleus, where β-catenin stimulates production of proteins necessary for cell cycle progression. Western blot analysis showed slight downregulation of P9GSK3β with BBS2 indicating downregulation of *wnt* signaling in BBS2 KO. Cyclin D1 was also probed for on the western blot because it is a target gene of the *wnt* signaling pathway, and it is only transcribed if canonical *wnt* signaling occurs. Cyclin D1 levels appeared to be much less on the western blot, indicating that canonical *wnt* signaling is being disrupted.

At the beginning of the canonical *wnt* signaling pathway, wnt activates receptor LRP 5/6. *In vitro* knockdown of BBS2 showed significantly reduced levels of LRP 5/6, indicating that BBS2 affects the *wnt* signaling pathway early on. Active β-catenin was also downregulated in BBS2 knockdown. Active β-catenin is a nuclear protein involved in the complex that allows transcription of wnt target genes to occur. Analysis showed that active β-catenin levels were significantly lower with BBS2 knockdown. Significantly lower levels of LRP 5/6 and active β-catenin combined with the apparently lower levels of total β-catenin, P9 GSK3β, and Cyclin D1 indicate that BBS2 knockdown leads to downregulation of the canonical *wnt* signaling pathway.

Depletion of BBS2 in β–Cells Results in S-Phase Arrest

In addition to being a target gene of the canonical *wnt* signaling pathway, Cyclin D1 is a cell cycle progression marker, so the decreased levels of Cyclin D1 seen with BBSS2 knockdown indicated cell cycle arrest. To determine whether or not cell cycle arrest occurred with BBS2 knockdown a FACS analysis was performed to determine which stage of the cell cycle siBBS2 transfected cells were in (**Figure 16**).

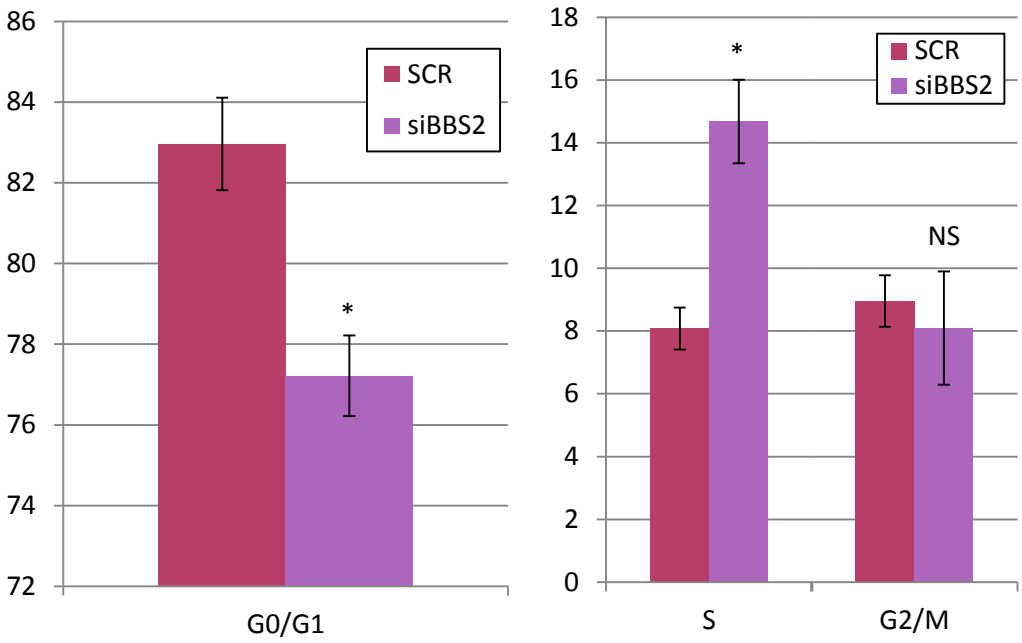

Figure 16: BBS2 knockdown results in s-phase arrest of β-cells. FACS cell cycle analysis was performed on BBS2 knockdown cells. Significantly more cells transfected with SCR were found to be in the G0/G1 phases of the cell cycle. Compared to the control, siBBS2 cells spent significantly more time in the s-phase of the cell cycle. The high percent of siBBS2 cells in the s-phase imply that BBS2 knockdown causes s-phase cell cycle arrest.

The FACS analysis of siRNA transfected cells showed that most SCR cells were in either the G0 or G1 phase of the growth cycle. Significantly fewer siBBS2 cells were found to be in the G0/G1 phases; instead, the siBBS2 cells were found to be in the s-phase of the cell cycle. There was no statistical difference in the percent of cells found in the G2 or M. The large difference in which stage of the cell cycle siBBS2 cells were in compared to the control indicates that cell cycle arrest occurs, and that BBS2 knockdown causes cells to become stuck in the s-phase.

DISCUSSION

Main Conclusions

The complications associated with Bardet-Biedl Syndrome indicate how important primary cilia are in the human body. The high frequency of obesity and type II diabetes among BBS patients has recently drawn attention to the syndrome as a potential way to better understand developmental and signaling pathways involved in the onset of these diseases. This project explored how the loss of BBS2 gene function affected glucose homeostasis and the length of primary cilia in pancreatic islet cells. It also examined the effect of BBS2 knockdown on the canonical *wnt* signaling pathway, known to be involved in adipogenesis repression, and cell cycle progression.

BBS2 knockout mice showed glucose intolerance but normal insulin resistance. The glucose tolerance test showed glucose intolerance, and plasma insulin level measurements indicated that BBS2 knockout animals have low blood insulin levels compared to the wild type. The insulin tolerance test showed similar insulin sensitivities between the BBS2 knockouts and the wild type; however, the knockouts were unable to stabilize their blood glucose levels in response to high insulin levels.

Morphological stains of pancreatic tissue from BBS2 knockouts had significantly lower insulin levels in the islets, supporting the potential for BBS2 knockouts to be insulin deficient. The perifusion results agreed with the idea of low insulin levels in BBS2 knockouts, who throughout the perifusion hyposecreted insulin in response to glucose stimulation and had lower total insulin levels. While typically glucose intolerance is compensated for with increased insulin levels, the BBS2 knockouts did not appear to

have this ability, indicating that their ability to produce insulin could be compromised in complete BBS2 KO since the Hets were still able to hypersecrete insulin.

Pancreatic islets from BBS2 knockout mice were stained for pericentrin, a centrosome marker, and acetylated tubulin to show the presence or absence of primary cilia in the islets. Islets from BBS2 knockouts clearly had fewer, shorter, and less organized cilia than the wild type. The wild type cilia are clearly discernible in Figure 12E. However, the BBS2 knockout cilia in Figure 12G were disorganized and aggregated, making them indiscernible in some areas. Although the wild type contained predominantly medium length cilia (64.3%) and fewer short cilia (30.7%), the BBS2 knockouts contained mostly short cilia (61.7%) and fewer medium length cilia (34.1%). This distinct BBS2 knockout phenotype of short, atypical cilia fits with the literature that BBS is a ciliopathy so patients have cilia that are either structurally impaired.

Knockdown of BBS2 was accomplished *in vitro* using rat insulinoma cells transfected with siRNA against BBS2. The *in vitro* knockdown confirmed lower insulin levels among BBS2 knockdown compared to the control, and supporting the *in vivo* findings that loss of BBS2 results in compromised insulin levels. In addition to determining how insulin levels were affected by BBS2 knockdown, various proteins involved in the canonical *wnt* signaling pathway were observed in the same way. The role of the canonical *wnt* signaling pathway in adipogenesis repression indicated it as a signaling pathway with the potential to play a role in the presence of obesity among BBS patients.

This project was able to show significant downregulation of *wnt* signaling proteins LRP 5/6 and active β-catenin and their target Cyclin D1 due to BBS2

knockdown. There appeared to be downregulation of two other *wnt* proteins and a *wnt* signaling target gene as well; total β-catenin, phosphor-9 GSK3β, and Cyclin D1 were all observed in lower levels in BBS2 knockdown compared to the control. Cyclin D1, a target gene of the canonical *wnt* signaling pathway, is a cell cycle progression marker. When a FACS cell cycle analysis was performed on BBS2 knockdown cells, it was discovered that knockdown of BBS2 results in s-phase arrest.

This finding fits with the abnormally few cilia seen in the BBS2 knockout islets compared to the wild type. When cells enter the cell cycle, they retract their primary cilia. Accordingly, if a higher number of BBS2 knockout cells are arrested in the s-phase of the cell cycle, they would not have cilia, giving a plausible explanation for the low number of cilia seen in the islet stains.

Research Complications

The most challenging problem encountered throughout this project was the small number of BBS2 knockout mice available for testing. Although BBS2 knockout mice were born, their small body sizes and poor health often lead to death before they were old enough to be used in experiments such as the glucose tolerance test, insulin tolerance test, and perifusion. All of these experiments were n = 2, and they should be repeated with a larger population. Despite the small population used in these experiments, the fact that all of the tests performed pointed to the conclusion that loss of BBS2 leads to glucose intolerance and low levels of insulin indicates that the results describe a BBS phenotype.

Future Research

In addition to performing the glucose tolerance test, insulin tolerance test, and perifusion with more mice, a better understanding of the link between BBS2 and obesity and diabetes would come from performing a variety of other experiments. The idea that

BBS2 knockdown causes cell cycle arrest should be verified with several other cell cycle progression markers, including a BrdU assay, KI67 staining, a tunnel assay, and a phosphohistone H3 assay. BrdU will allow the fate of the cell to be determined, specifically if cells are arrested in the s-phase. If a Tunel assay is used as a follow-up, it will be possible to determine if the arrested cells eventually undergo apoptosis or if they are able to eventually exit the cell cycle.

Somatostatin receptor 3 (SSTR3) is a protein involved in the secretion of hormones such as insulin. Since low plasma insulin levels were seen in this project, it would be interesting to discover if SSTR3 is localized to the cilia of pancreatic islets. The presence of SSTR3 on the primary cilia could influence the ability of the islets to secrete insulin, and thus explain the insulin hyposecretion seen in the perifusion performed on the BBS2 knockout islets.

The downregulation of several canonical *wnt* signaling proteins was observed throughout this project, and it would be interesting to discover whether or not other canonical *wnt* signaling genes were downregulated as well. This could easily be performed *in vitro*, and would confirm or deny the idea that BBS2 plays a role in canonical *wnt* signaling. While the canonical *wnt* signaling pathway represses adipogenesis, the non-canonical *wnt* signaling pathway is involved in adipogenesis. The two pathways are antagonistic, so non-canonical *wnt* signaling genes should be examined, and upregulation of these genes would be expected.

BIBLIOGRAPHY

Abcam Wnt signaling pathway [Online] // Abcam. - 2012. - PDF. - April 23, 2013. - http://docs.abcam.com/pdf/stemcells/Wnt-signaling-pathway.pdf.

Alberts Bruce [et al.] An Overview of the Cell Cycle [Book]. - New York : Garland Science, 2002. - Vol. 4th edition.

Badano Jose L [et al.] The Ciliopathies: An Emerging Class of Human Genetic Disorders [Journal] // Annual Review of Genomics and Human Genetics. - September 2006. - Vol. 7. - pp. 125-148.

Baker Kate and Beales Philip L Making sense of cilia in disease: The human ciliopathies [Journal] // American Journal of Medical Genetics. - November 15, 2009. - 4 : Vol. 151C. - pp. 281-295.

Cano David A [et al.] orpk mouse model of polycystic kidney disease reveals essential role of primary cilia in pancreatic tissue organization [Journal] // Development. - July 2004. - 14 : Vol. 131. - pp. 3457-3467.

Cell Cycle p21, Depression, and Neurogenesis in the Hippocampus [Blog Entry]. - [s.l.] : Sciencetopia Blogs, May 31, 2010.

Chiang Annie P [et al.] Homozygosity mapping with SNP arrays identifies TRIM32, an E3 ubiquitin ligase, as a Bardet-Biedl syndrome gene (BBS11) [Journal] // PNAS. - April 2006. - 16 : Vol. 103. - pp. 6287-6292.

Christensen Soren T [et al.] Sensory Cilia and Integration of Signal Transduction in Human Health and Disease [Journal] // Traffic. - February 2007. - 2 : Vol. 8. - pp. 97-109.

Christodoulides Constantinos [et al.] Adipogenesis and WNT signalling [Journal] // Trends in Endocrinology & Metabolism. - January 2009. - 1 : Vol. 20. - pp. 16-24.

Dai D [et al.] Planar cell polarity effector gene Intu regulates cell fate-specific differentiation of keratinocytes through the primary cilia [Journal] // Cell Death & Differentiation. - January 2013. - 1 : Vol. 20. - pp. 130-138.

Forsythe Elizabeth and Beales Philip L Bardet-Biedl Syndrome [Journal] // European Journal of Human Genetics. - 2013. - 1 : Vol. 21. - pp. 8-13.

Frank Valeska [et al.] Mutations of the CEP290 Gene Encoding a Centrosomal Protein Cause Meckel-Gruber Syndrome [Journal] // Human Mutation. - January 2008. - 1 : Vol. 29. - pp. 45-52.

Friedman Jeffrey M The Function of Leptin in Nutrition, Weight, and Physiology [Journal] // Nutrition Reviews. - September 2008. - Supplement s10 : Vol. 60. - pp. S1-S14.

Goto Hidemasa, Inoko Akihito and Inagaki Masaki Cell cycle progression by the repression of primary cilia formation in proliferating cells [Journal] // Cellular and Molecular Life Sciences. - March 2013.

Gromley Adam [et al.] Centriolin Anchoring of Exocyst and SNARE Complexes at the Midbody Is Required for Secretory-Vesicle-Mediated Abscission [Journal] // Cell. - October 2005. - 1 : Vol. 123. - pp. 75-87.

Guo DF and Rahmouni K Molecular basis of the obesity associated with Bardet-Biedl syndrome [Journal] // Trends in Endocrinology and Metabolism. - July 2011. - 7 : Vol. 22. - pp. 286-293.

Hamid HA Dandy-Walker Malformation [Journal] // Egyptian Journal of Medical Human Genetics. - 2007. - 2 : Vol. 8. - pp. 115-120.

Jin Hua and Nachury Maxence V The BBSome [Journal] // Current Biology. - June 2009. - 12 : Vol. 19. - pp. R472-R473.

Lee Brian H [et al.] Hyperactive Neuroendocrine Secretion Causes Size, Feeding, and Metabolic Defects of C. elegans Bardet-Biedl Syndrome Mutants [Journal] // PLoS Biology. - December 2011. - 12 : Vol. 9.

Locke Matthew [et al.] TRIM32 is an E3 ubiquitin ligase for dysbindin [Journal] // Human Molecular Genetics. - 2009. - 13 : Vol. 18. - pp. 2344-2358.

Mockel A [et al.] Retinal dystrophy in Bardet-Biedl syndrome and related syndromic ciliopathies [Journal] // Progress in Retinal and Eye Research. - July 2011. - 4 : Vol. 30. - pp. 258-274.

Otto Edgar A and al. et Candidate exome capture identifies mutation of SDCCAG8 as the cause of a retinal-renal ciliopathy [Journal] // Nature Genetics. - 2010. - Vol. 42. - pp. 840-850.

Parker David C [et al.] Survival of mouse pancreatic islet allografts in recipients treated with allogeneic small lymphocytes and antibody to CD40 ligand [Journal]. - PNAS : [s.n.], 1995. - 21 : Vol. 92. - pp. 9560-9564.

Pedersen Lotte B [et al.] Assembly of Primary Cilia [Journal] // Developmental Dynamics. - 2008. - pp. 1993-2006.

Quarmby Lynne M and Parker Jeremy D.K. Cilia and the Cell Cycle? [Journal] // The Journal of Cell Biology. - June 2005. - 5 : Vol. 169. - pp. 707-710.

Saade Carole J, Alvarez-Delfin Karen and Fadool James M Rod Photoreceptors Protect from Cone Degeneration-Induced Retinal Remodeling and Restore Visual Responses in Zebrafish [Journal] // The Journal of Neuroscience. - January 2013. - 5 : Vol. 33. - pp. 1804-1814.

Seo Seongjin [et al.] BBS6, BBS10, and BBS12 form a complex with CCT/TRiC family chaperonins and mediate BBSome assembly [Journal] // PNAS. - January 2010. - 4 : Vol. 107. - pp. 1488-1493.

Sheffield Val C The Blind Leading the Obese: The Molecular Pathophysiology of a Human Obesity Syndrome [Journal] // Transactions of the American Clinical and Climatological Association. - 2010. - Vol. 121. - pp. 172-182.

Singla Veena and Reiter Jeremy The Primary Cilium as the Cell's Antenna: Signaling at a Sensory Organelle [Journal] // Science. - 2006. - 5787 : Vol. 313. - pp. 629-633.

Valentine Megan Smith [et al.] Paramecium BBS genes are key to presence of channels in Cilia [Journal] // Cilia. - September 2012. - 1 : Vol. 1. - pp. 1-16.

Wei Qing [et al.] The BBSome controls IFT assembly and turnaround in cilia [Journal] // Nature Cell Biology. - August 2012. - Vol. 14. - pp. 950-957.

Wheatley Denys N and Bowser Samuel S Length control of primary cilia: analysis of monociliate and multiciliate PtK1 cells [Journal] // Biology of the Cell. - December 2000. - 8-9 : Vol. 92. - pp. 573-582.

Wheatley Denys N, Wang Ai Mei and Strugnell Gillian E Expression of Primary Cilia in MammalianCells [Journal] // Cell Biology International. - 1996. - 1 : Vol. 20. - pp. 73-81.

Wheway G [et al.] MKS1 interacts with components of the ubiquitin-proteasome pathway to regulate ciliogenesis and multiple signalling pathways // Poster presentation. - London, UK : Cilia, November 16, 2012. - Vol. 1.

Willaredt Marc A [et al.] A Crucial Role for Primary Cilia in Cortical Morphogenesis [Journal] // The Journal of Neuroscience. - November 2008. - 48 : Vol. 28. - pp. 12887-12900.

Yokoyama Takahiko Motor or sensor: A new aspect of primary cilia function [Journal] // Anatomical Science International. - June 2004. - 2 : Vol. 79. - pp. 47-54.

Zhang Qihong [et al.] Bardet-Biedl syndrome 3 (Bbs 3) knockout mouse model reveals common BBS-associated phenotypes and Bbs3 unique phenotypes [Journal] // PNAS. - December 2011. - 51 : Vol. 108. - pp. 20678-20683.